A Poisson Multi-Bernoulli Mixture approach to tracking trains using Distributed Acoustic Sensing

Marco Fontana*, Thomas Hayder‡, William Freilinger‡, Ángel F. García-Fernández*†, Simon Maskell*
*Dept. of Electrical Engineering and Electronics, University of Liverpool, United Kingdom
‡Sensonic GmbH, Schärding, Austria
†ARIES Research Centre, Universidad Antonio de Nebrija, Madrid, Spain
Emails: marco.fontana@liverpool.ac.uk, thomas.hayder@sensonic.com, william.freilinger@sensonic.com
angel.garcia-fernandez@liverpool.ac.uk, s.maskell@liverpool.ac.uk

***Abstract*—This paper presents an extended target tracking method to track trains using Distributed Acoustic Sensing (DAS) data. The problem is approached using a measurement likelihood based on a Set of Points on a Rigid Body (SPRB) model applied to a clustered version of the Poisson Multi-Bernoulli Mixture filter. The method efficiently handles asymmetric noise within the set of measurements returned by each train, and proposes a solution to merged measurements appearing at crossings. We use experimental data obtained from trains to show that the proposed algorithm has lower localisation and false target error, leading to better performance in terms generalized optimal sub-pattern assignment (GOSPA) metric.**

***Index Terms*—Random finite sets, Bayesian estimation, extended multi-target tracking, Poisson multi-Bernoulli mixtures.**

I. Introduction

Multiple target tracking (MTT) refers to the sequential estimation of both the number and the states of multiple dynamic targets, based on sensor measurements characterised by noise [1]. Traditional MTT algorithms are designed under the assumption of 'point target', wherein each target is represented as a spatially unextended point, and each target generates, at most, a single measurement per time step. Nevertheless, the point target assumption can become impractical with contemporary high-resolution sensors. These advanced sensors often lead to a scenario where a single target produces multiple measurements in a single scan, depending on the sensor type, target's position relative to the sensor, and the orientation of the target [2].

In this context, an extended target can be modelled as a group target, which is characterised as a cluster of point targets that cannot be individually tracked. For example, the sensor may be able to distinguish individual features or measurement sources of an extended target, therefore they must be collectively treated as a singular object. An intuitive strategy to address this challenge is to model the target as a rigid (or semi-rigid) set of point sources, with each source representing the point of origin of a sensor measurement [3]–[7]. Within the context of extended target tracking, the availability of multiple measurements enables the estimation of not only the target's position and kinematics, but also the target's extent in the measurement domain.

This work is supported by Sensonic GmbH.

Random Finite Sets (RFS) [8] offer an elegant Bayesian framework for formulating the MTT problem, paving the way for the development of multitarget conjugate priors in recent years. The Poisson multi-Bernoulli mixture (PMBM) is a conjugate prior [9] with Poisson birth model, which can handle both point targets [10] and extended targets [11], [12] and also targets with general-distributed measurements, e.g. to accommodate both point and extended targets, and the measurement model coming from an extended target modelled as a set of point sources [13]. The PMBM filter has also been extended to the clustered PMBM filter [14]. The clustered PMBM filter considers the union of a number of multi-Bernoulli mixtures (one multi-Bernoulli mixture for each cluster) for faster computation and successfully handling large scale problems.

In this paper, we consider tracking trains using Distributed Acoustic Sensing (DAS) data, which can detect the vibrations generated by a moving train by turning an optical fibre into an array of sensing units [15]. Unlike axle counters and balises, DAS provides continuous monitoring along the railway by using only an optical fibre cable and an interrogator. The spatial resolution is in the order of a few meters, depending on the length of the system, which can extend up to 80 km, and the data rate set by the interrogator at the end of the fibre.

Additionally, DAS has the advantage of reusing existing telecommunication fibre deployed alongside the railway track, thereby reducing installation and maintenance costs, with the interrogator being the only active element of the system. Therefore, DAS proves advantageous in challenging environments, such as rural or underground settings, where limited connectivity or access to satellite geolocalisation renders other alternatives less viable. Finally, DAS provides valuable information about the railway surroundings, offering useful insight into track conditions, third-party activities and occurrences of landslides. An accurate estimation of the train location is necessary to correctly analyse the DAS data and classify each portion of the signal appropriately.

Figs. 1 and 2 show, respectively, an example of DAS data showing a few train trajectories in a spatio-temporal map, often called a waterfall, and a schematic representing the typical configuration of a DAS system for train tracking. At each time step, train's vibrations are detected in a set of adjacent

sensing units localised between the head and the tail on the train, and only the locations of these two are returned by the detector and defined as edge measurements. We assume each train generates up to one pair of edge measurements at each time step, and we refer to it simply as target measurement or measurement.

Closely spaced trains can result in merged target measurements because one of the ends of the train is occluded by another train, as shown in Fig. 3. This scenario makes data association more complicated, as edge measurements in a target measurement are generated from different targets, and information about the train extent is lost. In the literature, Lagrangian relaxation methods can be employed to deal with merged measurements [16]. Other approaches were presented in [17], [18].

Another challenge is that edge measurements are affected by two distinct sources of uncertainty, i.e., uncertainty about the location of measurement sources relative to the centre of mass of the train, and uncertainty related to the dynamics of the train, expressed by the measurement noise. The latter is common to both the edge measurements of a train, and can be encapsulated in the density of the target state. The former kind of uncertainty results in an edge-dependent noise, as the distribution of the edge measurements around the locations of the ends of the train depends on several factors, the most important being the location of the locomotive along the train.

The stronger vibrations produced by the heavy weight and the engine of the locomotive result in a lower measurement noise of the edge measurements where the locomotive is located. Fig. 4 shows two examples of measurements produced by trains with the locomotive at the front of the train, where the related edge measurements (in green) show a temporal evolution that better describes the real dynamics of the trains.

As the use of the push-pull train configuration is common in most developed countries, it is not know a priori whether the locomotive is placed at the front or at the back of the train. Therefore, it is not possible to define an accurate characterisation of the edge measurement noise. Moreover, the length of the trains is unknown and can differ greatly depending on the type of train, i.e., passenger trains are generally much shorter than freight trains.

In this paper, we propose a model that assumes a symmetric edge measurement noise and discards highly noisy edge measurements. The aim of this work is to locate the ends of the trains at each time step by estimating both the location of the centre of mass and the length of the trains. The main contribution of this work is the extension of the clustered PMBM filter [14] for tracking multiple trains based on detections obtained from DAS data. The proposed clustered PMBM filter is designed to deal with asymmetric edge measurement noise and independent data association of each edge measurement in case of merged target measurement.

The remainder of the paper is organised as follows. Sec. II presents the problem by specifying the assumptions on the measurements, the proposed model for the extended target state and the measurement sources. Sec. III introduces an overview of the proposed solution by describing the extended target measurement model, along with the multi-target likelihood and the PMBM posterior. Section IV presents more details about the filtering recursion, and Sec. V introduces a cluster-based method to compute the data association in scenarios with merged measurements. Sec. VI presents a comparison based on real DAS data between the proposed extended target PMBM filter and the point-target clustered PMBM filter presented in [14]. Finally, Sec. VII draws the conclusions and suggests possible future lines of research.

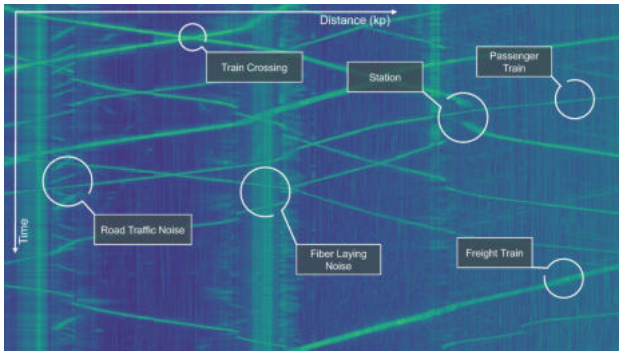

Figure 1: Example of a DAS waterfall consisting of 11 train trajectories produced by trains of different kind and size. The x-axis represents the distance from the interrogator in kilometre point (kp), while the y-axis shows the time.

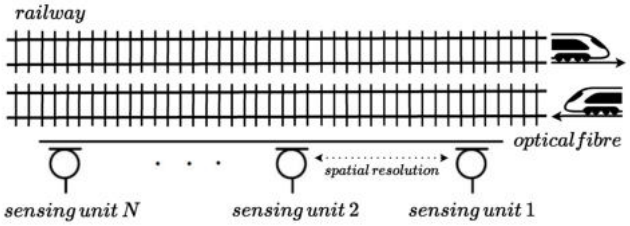

Figure 2: Schematic of the DAS system configuration in a train tracking scenario. The fibre is placed following two parallel train tracks with trains moving in opposite directions. Each sensing unit measures a noisy acoustic energy signal from nearby trains.

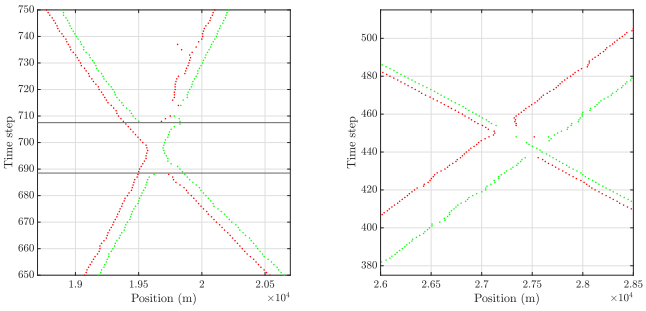

Figure 3: Two examples of edge measurements of two trains travelling in different directions and meeting at the centre of the plot, where their signals overlap and the detector returns merged measurements. Each point represents an edge measurement (z, ℓ), where the red ones are associated with the descriptor tag $\ell = l$ and the green one with $\ell = r$. In the figure on the left-hand side, the two trains have approximately the same length, and the merged measurements are confined between the two horizontal black lines. The figure of the right-hand side shows a scenario with two trains of different length, where the merged and non-merged measurements are mixed.

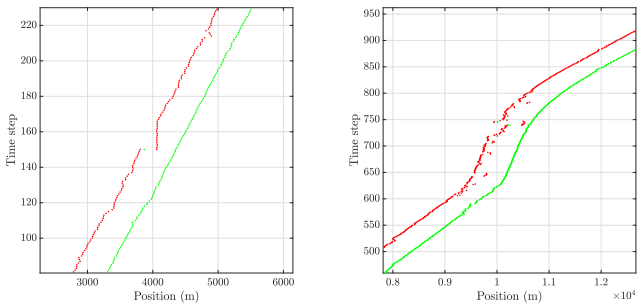

Figure 4: Two examples of edge measurements affected by different noise intensity. The figure on the left hand side shows possible artefacts affecting the left edge measurements of the train. On the right hand side, the figure shows the left edge measurements affected by noise resembling a Gaussian distribution.

II. Problem formulation

In this section we introduce the extended train state and some assumptions on the target measurements and edge measurements. Some of these assumptions will be expanded in Sec. V to define the data association problem with merged measurements. As the shape of the target is one-dimensional, we choose to represent both the kinematics and the extent of the target in one vector. We also define the concept of measurement sources to describe the locations where the edge measurements are generated.

A. Edge and target measurements

Each train generates a signal that spans over several sensing units, as the sensor has a resolution in the order of a few meters. A detector classifies the output of each sensing unit either as 'no train' or 'train signal', and sequences of contiguous units labelled as 'train signal' are identified as singular target measurements at each time step. DAS data and detector's segmentation are displayed in waterfall plots with position and time on the x and y axes, respectively, as shown in Figs. 1, 3 and 4.

For each target measurement, the detector returns a pair of measurements corresponding to the leftmost and the rightmost sensing units labelled as 'train signal', representing the location of the head and the tail of the train. We refer to the left and right measurements as edge measurements (as they locate the edges of the signal), and we denote them as (z, l) and (z, r), respectively. At time step k, the detector returns a set of n_k target measurement $\mathbf{Z}_k = \{Z_k^i\}_{i=1}^{n_k}$. Each element of $\mathbf{Z}_k$ is a set of edge measurements $(z_j, \ell_j) \in \mathbb{R} \times \{l, r\}$, i.e., $Z_k^i = \{(z_j, \ell_j)\}_{j=1}^{n(Z_k^i)}$, where ℓ_j is a descriptor tag assigned by the detector and $n(Z_k^i)$ is the number of edge measurements assigned to Z_k^i by the detector. Note that tags allow us to implicitly address the association problem between the edge measurements and the two ends of the train without the need for additional computations.

The assumptions on the multitarget measurement process are:

- Each train generates up to one set of edge measurements Z_k at each time step.
- If the trains are sufficiently spaced, each target measurement is the result of at most one train.
- Each end of the train generates up to one edge measurement (z_j, ℓ_j), i.e., each train generates up to two edge measurements at each time step.
- Each edge measurement is the result of at most one train.

It is worth noting that the target measurements returned by the detector represent a partition of the set of edge measurements, where each subset is a target measurement defined by $Z_k = \left\{\left(z_k^1, l\right), \left(z_k^2, r\right)\right\}$ such that, for any $\left(z_k^1, l\right)$, $\left(z_k^2, r\right)$ is the right edge measurement with minimum distance from z^1, and vice versa. Discarding all the other possible partitions of the edge measurements results in a sensible simplification of the problem.

B. Extended target state

Because the sensor is oriented parallel to the railway, we can assume the train being a rigid body form the sensor point of view. Therefore, the two ends of the train have unified dynamics, i.e., move with the same speed v_k. A detection originating from the head of the train contains information about the tail, and vice versa. The positions x_k^l and x_k^r of the ends of the train, denoted in analogy with the edge measurements, are related to the location of its centre of mass x_k^c by the train length o_k. In this work, the target state x_k is chosen to be

$$x_k = [x_k^c, v_k, o_k]^T , \tag{1}$$

and we aim to estimate the locations of the head and tail of the trains defined by the extended target state components, namely x_k^c and o_k. Analogously to the set of edge measurements Z_k, we denote a set of extended target states at time step k as $X_k \in \mathcal{F}(\mathcal{X})$, where $\mathcal{F}(\mathcal{X})$ represents the set of finite subsets of $\mathcal{X}$.

Each edge measurement (z_k, ℓ) can be seen as a measurement source that is measured with some noise w_k^ℓ

$$z_k = H^\ell x_k + w_k^\ell \tag{2}$$

where w_k^ℓ is an independent zero-mean Gaussian measurement noise with variance σ_ℓ^2, and H^ℓ with $\ell \in l, r$ is

$$H^l = \begin{bmatrix} 1 & 0 & -1/2 \end{bmatrix} \qquad H^r = \begin{bmatrix} 1 & 0 & 1/2 \end{bmatrix} . \tag{3}$$

The likelihood of the edge measurement (z, ℓ) given the extended target state x_k is

$$p^\ell(z_k | x_k) = \mathcal{N}(z_k; H^\ell x_k, \sigma_\ell^2) . \tag{4}$$

III. Overview of the solution

In this section we define an extended target measurement model tailored to our specific problem, and we provide its multi-target derivation. Later we describe the PMBM posterior density and its clustered version [14], highlighting key aspects of their characteristics.

A. Extended target measurement model

Each train can be represented as an extended object with $L = 2$ measurement sources[1] located on a rigid body shape, i.e. at the end of the train, using a Set of Points on a Rigid Body (SPRB) model [2] (also called Exact Rigid-Body (ERB) model [8]). The measurement sources are detected independently of each other, and the measurement source ℓ has a detection probability p_D^ℓ that is a function of the target state. The measurement likelihood is [8]

$$l(Z_k|x_k) = \sum_{\theta} \prod_{\theta_\ell=0} (1 - p_D^\ell) \prod_{\theta_\ell \neq 0} p_D^\ell p^\ell \left((z_k, \theta_\ell)\,|x_k\right) \quad (5)$$

if $|Z_k| \leq L$ and $l(Z_k|x_k) = 0$ otherwise. In this context, $\theta = \{\theta_l, \theta_r\} \in \Theta$ is an assignment variable with $\theta_l \in \{0, l\}$ and $\theta_r \in \{0, r\}$, such that each edge measurement can be associated with just one of the measurement sources. Therefore, the set Θ of possible associations detection-measurement source has cardinality $|\Theta| = 4$, and assuming $p_D^l = p_D^r = p_D$ as a constant, we can rewrite (5) using the likelihood of the edge measurement (4) as

$$l(Z_k|x_k) = \begin{cases} (1-p_D)^2 & Z_k = \emptyset \\ p_D(1-p_D)p^l(z_k|x_k) & Z_k = \{(z_k, l)\} \\ p_D(1-p_D)p^r(z_k|x_k) & Z_k = \{(z_k, r)\} \\ p_D^2 p^l(z_k^1|x_k)p^r(z_k^2|x_k) & Z_k = \{(z_k^1, l), (z_k^2, r)\} \end{cases} \quad (6)$$

. We can formulate (6) as a multi-Bernoulli RFS

$$l(Z_k|x_k) = \sum_{Z_k^1 \uplus Z_k^2 = Z_k} f^1(Z_k^1|x_k) f^2(Z_k^2|x_k) \quad (7)$$

where each measurement source is described by a Bernoulli RFS

$$f^\ell(Z_k|x_k) = \begin{cases} 1 - p_D & \text{if } Z_k = \emptyset \\ p_D p^\ell(z_k|x_k) & \text{if } |Z_k|{=}1 \\ 0 & \text{otherwise.} \end{cases} \quad (8)$$

The measurement model proposed above allows us to discard one of the two edge measurements during the update of the target state. This proves beneficial in cases of sudden changes in the target length, i.e., example on the left in Fig. 4, as we can use the least noisy component of the target measurement to update the kinematic part of the target state without altering the estimation of the length.

B. Multi-target likelihood

The set of measurements $\mathbf{Z}_k$ is the union of a set of clutter measurements and the set of target generated measurements, with these two sets assumed independent. We model the clutter as a PPP with intensity $\lambda_c(\mathbf{Z}) = \lambda c(\mathbf{Z})$, where $c(\cdot)$ is the spatial distribution of the clutter measurements, and λ is the expected rate of clutter measurements. The multi-target measurement model is the union of a multi-Bernoulli RFS and Poisson RFS

$$p(\mathbf{Z}_k|X_k) = e^{-\lambda} \sum_{\boldsymbol{Z}^c \uplus \boldsymbol{Z}^1 \uplus \cdots \uplus \boldsymbol{Z}^n = \boldsymbol{Z}_k} [c(\cdot)]^{\boldsymbol{Z}^c}$$

$$\times \prod_{i=1}^{n} \sum_{\uplus_{j=1}^{n(Z_k)} Z_k^j = \boldsymbol{Z}^i} \sum_{Z_k^1 \uplus Z_k^2 = Z_k} f^1(Z_k^1|x_k^i) f^2(Z_k^2|x_k^i) \quad (9)$$

where the summation is taken over all mutually disjoint subsets $\boldsymbol{Z}^c, \boldsymbol{Z}^1, \ldots, \boldsymbol{Z}^n$ of $\boldsymbol{Z}$ (null set included) such that $\boldsymbol{Z}^c \cup \boldsymbol{Z}^1 \cup \cdots \cup \boldsymbol{Z}^n = \boldsymbol{Z}$, and $[c(\cdot)]^{\boldsymbol{Z}} = \prod_{Z \in \boldsymbol{Z}} c(\boldsymbol{Z})$, $[c(\cdot)]^{\emptyset} = 1$.

C. PMBM posterior

The Poisson Multi-Bernoulli (PMBM) density $f_{k|k'}(\cdot)$ of the set of targets at time step k' given measurements up to time step k results from the combination of two independent RFSs: a Poisson RFS with density $f_{k'|k'}^p(\cdot)$, and a multi-Bernoulli mixture (MBM) RFS with density $f_{k|k'}^{mbm}(\cdot)$, where $k' \in \{k-1, k\}$. The union of these two RFSs has been proved to be a conjugate prior with respect to the standard point target measurement model [9], [10]. The PMBM density is expressed over the union of the undetected targets set Y, and the detected target set W:

$$f_{k|k'}(X) = \sum_{Y \uplus W = X} f_{k|k'}^p(Y) f_{k|k'}^{mbm}(W) \quad (10)$$

where the sum goes over all mutually disjoint sets Y and W, which have the property that their union is X.

The Poisson RFS density represents the targets that exist at the current time instant, but have not yet been detected; it is defined as

$$f_{k|k'}^p(X) = e^{-\int \lambda_{k|k'}(x)dx} \prod_{x \in X} \lambda_{k|k'}(x) \quad (11)$$

where $\lambda_{k|k'}(\cdot)$ is the intensity of the Poisson RFS. In the PPP, the cardinality is Poisson distributed and targets are independent, and identically distributed. The MBM part represents the potentially detected targets, and it can be described as [9]:

$$f_{k|k'}^{mbm}(X) = \sum_{a \in \mathcal{A}_{k|k'}} w_{k|k'}^a \sum_{\uplus_{j=1}^{n_{k|k'}} X^j = X} \prod_{i=1}^{n_{k|k'}} f_{k|k'}^{i,a^i}(X^i) \quad (12)$$

where i is the index over the Bernoulli components, $a = \{a^1, \ldots, a^{n_{k|k'}}\} \in \mathcal{A}_{k|k'}$ represents a specific data association hypothesis, $a^i \in \{1, \ldots, h_{k|k'}^i\}$ is an index over the $h_{k|k'}^i$ single target hypotheses for the i-th potential target/Bernoulli component, and $n_{k|k'}$ is the number of potentially detected targets. Each set of single target hypothesis $a \in \mathcal{A}_{k'|k}$ is also called a global hypothesis, and it is associated to a weight $w_{k|k'}^a$ satisfying $\sum_{a \in \mathcal{A}_{k|k'}} w_{k|k'}^a = 1$. The same single target hypothesis can appear in several global hypotheses.

The Bernoulli density corresponding to the i-th potential target and the a_i single target hypothesis $f_{k|k'}^{i,a^i}(X)$ can describe a newly detected target, or it can represent a previously detected target or clutter; it makes it possible to efficiently model both the uncertainty regarding target existence and state. Mathematically, it can be expressed as

$$f_{k|k'}^{i,a_i}(X) = \begin{cases} 1 - r_{k|k'}^{i,a^i} & X = \emptyset \\ r_{k|k'}^{i,a^i} p_{k|k'}^{i,a^i}(x) & X = \{x\} \\ 0 & \text{otherwise} \end{cases} \quad (13)$$

[1] In a radar context, measurement sources are often called scattering/reflection points or sources, depending on whether the reflector is a discrete point or a larger structure.

where $r^{i,a^i}_{k|k'} \in [0,1]$ is the probability of existence and $p^{i,a^i}_{k|k'}(\cdot)$ is the state density given that it exists. In this work, we consider the Gaussian implementation proposed in [10], where $p^{i,a^i}_{k|k'}(x) = \mathcal{N}(x; \mu^{i,a^i}_{k|k'}, P^{i,a^i}_{k|k'})$, with mean $\bar{x}^{i,a^i}_{k|k'}$ and variance $P^{i,a^i}_{k|k'}$. In this context, the MBM is entirely defined by the following parameters:

$$\{(w^a_{k|k'}, r^{i,a^i}_{k|k'}, \mu^{i,a^i}_{k|k'}, P^{i,a^i}_{k|k'})\}_{i\in\{1,\dots,n_{k|k'}\}} \tag{14}$$

where $a \in \mathcal{A}_{k|k'}$ is defined above.

D. Clustered approximation of the PMBM posterior

To introduce the clustered PMBM approximation, it is useful to revisit the concept of auxiliary variable, wherein the target state x is augmented with a variable $u \in \mathbb{U}_{k|k'}$, such that (u, x). Here, $u = 0$ denotes an undetected target, while $u = i$ indicates that the target x originates from the i-th Bernoulli component. For further mathematical insights, refer to [19]. We denote multi-target densities and variables with auxiliary variables with a tilde, i.e., $\widetilde{f}_{k|k'}(\cdot)$ and $\widetilde{X}^i$, respectively.

The clustered approximation of the PMBM density $\widetilde{f}_{k|k'}(\cdot)$ on the augmented space $\mathcal{F}\left(\mathbb{U}_{k|k'} \times \mathbb{R}^{n_x}\right)$ of sets of target states with auxiliary variables allow us to express the posterior on a set of n^c_k independent clusters $C^1_k, ..., C^{n^c_k}_k$. Each cluster C^c_k is a set of auxiliary variables corresponding to the tracks assigned to the cluster $c = \{1, \dots, n^c_k\}$. The clustered PMBM density is [14]

$$\widetilde{f}_{k|k'}\left(\widetilde{X}\right) = \widetilde{f}^0_{k|k'}\left(\widetilde{Y}\right) \prod_{c=1}^{n^c_k} \widetilde{f}^c_{k|k'}\left(\cup_{i\in C^c_k} \widetilde{X}^i\right) \tag{15}$$

where $\widetilde{Y}$ is the set of undetected targets with auxiliary variable $u = 0$ and density $\widetilde{f}^0_{k|k'}(\cdot)$, and

$$\widetilde{f}^c_{k|k'}\left(\cup_{i\in C^c_k} \widetilde{X}^i\right) = \sum_{a_c \in \mathcal{A}^c_{k|k'}} w^{a_c}_{k|k'} \prod_{i\in C^c_k} \widetilde{f}^{i,a^i}_{k|k'}\left(\widetilde{X}^i\right). \tag{16}$$

is the MBM density of the potential targets $\widetilde{X}^i$ in the cluster c, i.e., $i \in C^c_k$. Note that the set of data association hypotheses $\mathcal{A}^c_{k|k'}$ is cluster-dependent, as this formulation allows us to split the data association problem into n^c_k independent sub-problems. In the next sections of the paper, we will exclude the tildes from the clustered PMBM density and the augmented target states to enhance readability.

IV. PMBM FILTERING RECURSION

In this section, we present the filtering recursion of the clustered PMBM for the extended multiple target measurement model described in Sec. III-B. We implement a constant velocity and constant length transition model at the prediction step, and we compute several hypotheses out of each Bernoulli component by considering one, two or no edge measurements at the update step, according to (6).

A. Prediction

The prediction is performed as in the clustered PMBM on the extended target state x_{k-1}, i.e., both on the kinematics and the length of the target. For each PPP component and single-target hypothesis, we compute the extended target states at time k using the Kalman filter. We model each target state $x_k \in X_k$ using a linear Gaussian dynamic model

$$x_k = F x_{k-1} + w_k \tag{17}$$

where F is the transition matrix, and $w_k \sim \mathcal{N}(0, Q)$ is the process noise with noise covariance Q.

B. Update

The PMBM update for a measurement model of the form (7) is given by [13]. Here we present a practical update suitable for processing the DAS data. We define the notation

$$\langle a, b\rangle = \int a(x)b(x)dx \tag{18}$$

to indicate the inner product between two real-valued functions $a(\cdot)$ and $b(\cdot)$, and concisely report the update equations.

1) PPP update: The intensity of the PPP is [13]

$$\begin{aligned}\lambda_{k|k}(x) &= l\left(\emptyset|x\right)\lambda_{k|k-1}(x)\\ &= (1-p_D)^2\lambda_{k|k-1}(x)\,,\end{aligned} \tag{19}$$

where the predicted PPP intensity is multiplied by the likelihood of misdetecting both the edge measurements, according to the first case in (6).

2) Bernoulli update: For each Bernoulli component indexed by $a^i \in \{1, \dots, h^i_{k|k-1}\}$ and $i \in \{1, \dots, n_{k|k-1}\}$ and each target measurement in the set $\boldsymbol{Z}_k = \{Z^1_k, \dots Z^{m_k}_k\}$, the update step based on the target measurement model (6) results in three Bernoulli components and a total misdetection hypothesis.

Total misdetection hypothesis:

$$w^{i,a^i}_{k|k} = w^{i,a^i}_{k|k-1}\left[1 - r^{i,a^i}_{k|k-1} + r^{i,a^i}_{k|k-1}\left\langle f^{i,a^i}_{k|k-1}, (1-p_D)^2\right\rangle\right] \tag{20}$$

$$r^{i,a^i}_{k|k} = \frac{r^{i,a^i}_{k|k-1}\left\langle f^{i,a^i}_{k|k-1}, (1-p_D)^2\right\rangle}{1 - r^{i,a^i}_{k|k-1} + r^{i,a^i}_{k|k-1}\left\langle f^{i,a^i}_{k|k-1}, (1-p_D)^2\right\rangle} \tag{21}$$

$$f^{i,a^i}_{k|k}(X) = \frac{(1-p_D)^2) f^{i,a^i}_{k|k-1}(x)}{\left\langle f^{i,a^i}_{k|k-1}, (1-p_D)^2\right\rangle}\,. \tag{22}$$

Partial and total update: The new single target hypotheses for the Bernoulli component i, a^i and measurement Z^j_k have probability of existence $r^{i,a^i}_{k|k} = 1$ and

$$w^{i,a^i}_{k|k} = w^{i,a^i}_{k|k-1} r^i_{k|k-1}\left\langle f^{i,a^i}_{k|k-1}, l\left(Z^j_k|\cdot\right)\right\rangle \tag{23}$$

$$f^{i,a^i}_{k|k}(X) = \frac{l\left(Z^j_k|x\right) f^{i,a^i}_{k|k-1}(x)}{\left\langle f^{i,a^i}_{k|k-1}, l\left(Z^j_k|\cdot\right)\right\rangle}\,. \tag{24}$$

Depending on the type of target measurement Z^j_k, i.e., on the form of $l\left(Z^j_k|X\right)$, the update results in either case (a) or (b), as described below.

a) Partial misdetection: either the left or the right edge measurement is detected, and the target state is updated according to cases 2 and 3 in (6). Note that the length o_k in the target state x_k is only predicted, as a single measurement does not provide information on the train length.

b) Full detection: both the edge measurements are detected. Both the kinematic part and the length component o_k of the target state are updated according to the last case in (6).

New track: for a new Bernoulli component with index $i = n_{k|k-1} + j$ initiated by a measurement $Z_k^j = \left\{\left(z_k^1, l\right), \left(z_k^2, r\right)\right\}$ we can have either a misdetection or a detection. We propose a practical approach wherein the parameters of the new Bernoulli component in case of a detection are

$$w_{k|k}^{i,2} = \delta_2\left[|Z_k^j|\right]\left(\left[\prod_{\left(z_k^j,\ell\right)\in Z_k^j} \lambda_c\left(z_k^j\right)\right] + \left\langle \lambda_{k|k-1}, l\left(Z_k^j|\cdot\right)\right\rangle\right) \tag{25}$$

$$r_{k|k}^{i,2} = \frac{\left\langle \lambda_{k|k-1}, l\left(Z_k^j|\cdot\right)\right\rangle}{w_{k|k}^{i,2}} \tag{26}$$

$$f_{k|k}^{i,2}(X) = \frac{l\left(Z_{k+1}^j|x\right)\lambda_{k|k-1}(x)}{\left\langle \lambda_{k|k-1}, l\left(Z_k^j|\cdot\right)\right\rangle}, \tag{27}$$

where $\lambda_{k|k-1}(\cdot)$ is the intensity of the PPP that models the birth on new targets, and the Kronecker delta $\delta_i[j] = 1$ if $j = i$ and $\delta_i[j] = 0$, otherwise. The Kronecker delta in (25) implies that a new track is initialised only if the target measurement Z_k^j contains two edge measurements. Finally, in case of a misdetection, the parameters of the new Bernoulli component are $w_{k|k}^{i,1} = 1$, $r_{k|k} = 0$.

V. Data association with merged measurements

Trains travelling along parallel train tracks, each designated for a specific direction, occasionally happen to be at the same location for brief periods of time. In this case, the condition on the second assumption in Sec. II-A is not verified, and target measurements may be generated by multiple trains. In this section, we present a solution to solve the data association problem by relaying on the clustered PMBM approximation [14].

We restrict the more general concept of merged measurement to the train tracking scenario by formulating the following assumptions:

- The maximum number of parallel train tracks is 2.
- Trains travelling on parallel train tracks travel in opposite directions.
- Trains on the same train track travel at a safe distance in the order of hundreds of meters.

Under to these assumptions, we conclude that each target measurement is the result of at most two trains.

A. Data association modes

We define two different data association problems, based on the validity of the second assumption in Sec. II-A. In the normal mode, trains are sufficiently far apart and the pair of left and right edge measurements of each target measurement are generated by the same train. In this case, it is computationally effective to define the data association problem in the space of the target measurements.

In the closely-spaced mode, one of the train's signal is either entirely or partially occluded by another train, and the edge measurements paired by the detector may be originated by different trains. In this case, the data association problem must be defined in the space of the edge measurements, with the possibility of assigning left and right edges belonging to the same pair to different targets. In order to simplify the solution of the data association problem, we prevent the filter to update existing tracks using both edge measurements in a target measurement by setting to zero the likelihood (6) for $Z = \left\{\left(z_k^1, l\right), \left(z_k^2, r\right)\right\}$.

B. Measurement-driven clustering

The measurement-driven clustering algorithm in [14] considers the measurements associated to each Bernoulli component via gating procedure to determine clusters of potential targets and measurements. Each cluster is characterised by a cluster density (16) in the form of a MBM density, where each mixture component represents a so called global hypothesis, i.e. a possible solution of the data association problem for the measurements and potential targets in the cluster. Each cluster defines a self-contained data association problem at each time step, which can be defined according to the normal mode or the closely-spaced mode.

C. Data association mode identification

We identify a set of conditions to determine whether the second assumption in Sec. II-A is verified, and so the most appropriate data association mode for each cluster. In the normal mode, the assumption is verified and the cluster represents only one true target. The number of potential targets in the cluster tends to two [14], as it comprises for a long-standing updated track and a new one related to the same measurement. In general, each cluster may contain also a few tracks initiated in the previous time steps, survived to pruning due to high measurement noise or clutter intensity.

In the closely-spaced mode, each cluster contains more than one true target, i.e. two trains getting close. The number of long-standing updated tracks in each cluster is two, along with a newly born track and potentially several other recently born ones due to high of measurement noise and clutter intensity.

Therefore, it is possible to determine the most appropriated data association mode of each cluster by the number of long-standing updated tracks in it. The definition of long-standing is based on the difference between the initialisation time of the track and the current time step. If the difference is above a specific threshold defined by the user, the track is marked as a long-standing one and it is considered in the determination of the data association mode.

VI. Evaluation

In this section, we evaluate the extended target PMBM filter on two datasets with real experimental data in several scenarios, obtained via the DAS systems deployed by Sensonic GmbH in Austria, Brazil, Czech Republic, India, France and Egypt. These systems monitor various kinds of train traffic (freight and passenger, also on the same line), speed (up to 250 km/h and down to 30 km/h) and length (longer than 1 km and shorter than 50 m).

We proceed to describe the parameters and the configuration of the filter in this context. All units in this section are expressed in the international system and omitted for notational clarity. The PPP birth model is a Gaussian mixture with two components with opposite mean velocity, i.e., $[L/2, 20, 375]$ and $[L/2, -20, 375]$, and covariance $\mathrm{diag}([(L/2)^2, 400, 375^2])$, where L is the length of the DAS system. The total intensity of the PPP is 1 at the first time step and 0.05 afterwords. The transition matrix F and and the covariance of the process noise Q are

$$F = \begin{pmatrix} 1 & T & 0 \\ 0 & 1 & 0 \\ 0 & 0 & 1 \end{pmatrix} \qquad Q = q_d \begin{pmatrix} \frac{T^3}{3} & \frac{T^2}{2} & 0 \\ \frac{T^2}{2} & T & 0 \\ 0 & 0 & \frac{q_o}{q_d} \end{pmatrix}, \quad (28)$$

where $T = 0.896$ s is the time interval, $q_d = 0.5$ is the intensity of the kinematic noise and $q_o = 100$ is the process noise of the train length.

The clustered PMBM filter implementation [14] uses a threshold for pruning the Poisson components $\Gamma_p = 10^{-7}$, a threshold for pruning global hypotheses $\Gamma_{mbm} = 10^{-7}$, and a threshold for pruning Bernoulli components $\Gamma_b = 10^{-7}$. The maximum number of global hypotheses is $N_h^c = 20|C^c|$ for each cluster c in the filter. The ellipsoidal gating is performed with a k-d tree of threshold $\Gamma_g = 10$, while the estimation is performed selecting the global hypothesis with the highest weight and reporting Bernoulli components whose existence probability is above 10^{-3} [10, Sec. VI.A]. The intra-track Bernoulli merging procedure [14] has threshold $\Gamma_m = 2.5$ to determine similar Bernoulli components, and the threshold defining the long-standing tracks is $\Gamma_s = 20$ time steps. The parameters of the filter are set to minimise both false target error and track fragmentation.

1) Dataset 1: The first dataset comprises of 5 scenarios with a total duration time of 103 minutes, where each scenario contains up to 3 trains moving at the same time. The trains are well-spaced, and there are no merged measurements in the scenarios, as shown in the example in Fig. 5. The dataset contains real experimental data; however, no ground truth is available. For performance evaluation, the ground truth has been derived through visual inspection and manual annotation of the data, by marking one of the edges of the train and determining its length.

We compare the performance of the proposed extended target (clustered) PMBM filter with the clustered (point target) PMBM [14] using the generalized optimal sub-pattern assignment (GOSPA) [20] with parameters $\alpha = 2$, $c = 100$ m, and $p = 2$. It is expected that the proposed PMBM filter outperforms the clustered (point target) PMBM filter, as the measurements are not accurately modelled by a point target model. As the standard clustered PMBM is based on the point target assumption with no length estimation, we merge each pair of measurements corresponding to the two edges of the train into a single measurement located at the centre of the train. We compute the GOSPA metric using the estimated midpoint locations returned by both filters.

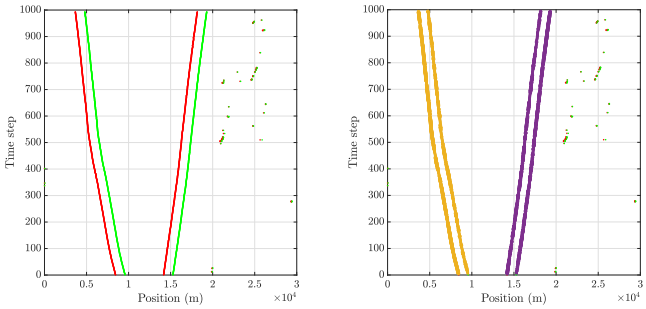

Figure 5: Scenario 2 in dataset 1. Each point in the figure on the left hand side represents an edge measurement z^ℓ, where the red ones are associated with the descriptor tag $\ell = l$ and the green one with $\ell = r$. The figure on the right hand side shows the the output of the proposed extended target PMBM filter, where the estimated locations of the ends of the trains are represented in yellow and purple.

Table I: Performance comparison between the clustered PMBM [14] and the proposed extended target PMBM filter in terms of RMS GOSPA error and its components. The best-performing method in each scenario is underlined.

Scenario	Clustered PMBM implementation	Total GOSPA	Localisation [m]	False target	Missed target
1	Extended target	<u>48.75</u>	35.69	23.49	23.49
	Point target	57.42	46.57	33.05	5.96
2	Extended target	<u>35.27</u>	33.37	8.08	8.08
	Point target	58.11	47.39	33.63	0
3	Extended target	<u>49.56</u>	36.86	23.43	23.43
	Point target	52.57	38.59	34.08	10.65
4	Extended target	<u>35.85</u>	27.33	16.4	16.4
	Point target	49.73	27.19	41.08	6.74
5	Extended target	<u>56.4</u>	27.9	34.66	34.66
	Point target	84.7	57.44	61.79	7.62

Tab. I shows the performance of the two filters in the 5 scenarios of dataset 1 in terms of total root mean square (RMS) GOSPA error and its components. The extended target PMBM filter outperforms the clustered PMBM filter in all scenarios of dataset 1. The proposed filter shows better performance both in terms of localisation error and false target error. The missed target error results higher in for the extended target PMBM filter due to longer track initiation times compared to the clustered PMBM. Fig. 5 shows measurements and outcomes of the proposed algorithm applied to scenario 2 in dataset 1, where clutter is correctly identified in the top right section of the plot.

2) Examples from dataset 2: The second dataset contains data about more challenging scenarios, where up to 7 trains

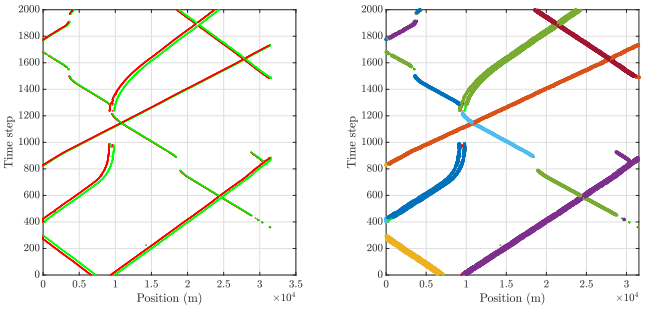

Figure 6: Example of a scenario in dataset 2. Each point in the figure on the left represents an edge measurement z^{ℓ}, where the red ones are associated with the descriptor tag $\ell = l$ and the green one with $\ell = r$. The figure on the right hand side shows the the output of the proposed extended target PMBM filter, where each colour represents a different auxiliary variable.

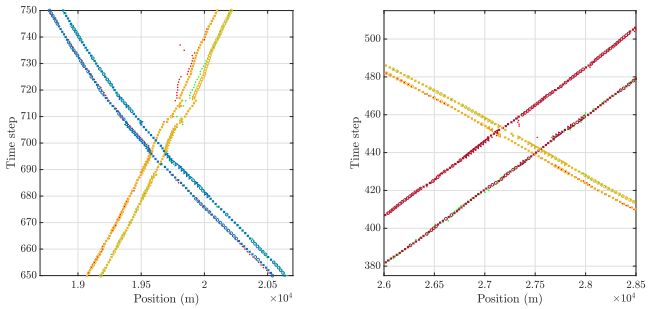

Figure 7: Output of the proposed extended target PMBM filter based on the measurements showed in Fig. 3.

move simultaneously, often approaching each other and resulting in merged measurements. As ground truth annotations are not available for this dataset, we proceed reporting a few key examples of the performance of the proposed filter. We omit the outcomes of the PMBM filter because it exhibits underperformance in this scenario, due to the high number of merged measurements.

Fig. 6 shows an example of a scenario in dataset 2, along with the output of the proposed extended target PMBM filter on the right-hand side. Each colour represent a different auxiliary variable in the PMBM filter. The filter shows good tracking performance and low track fragmentation, returning consistent auxiliary variables in the presence of merged measurements. Fig. 7 focuses on the output of the proposed extended target PMBM filter in the presence of merged measurements. The same scenarios were introduced in Fig. 3.

VII. Conclusion and Future Work

In this paper, we proposed a method to track trains using DAS data. We presented an extended multi target tracking algorithm based on the clustered PMBM filter, able to provide superior tracking performance and reduce track fragmentation. The SPRB model implemented in the algorithm allows the filter to efficiently deal with asymmetric edge measurement noise. We showed a method based on the clustered PMBM filter to solve the data association problem in each cluster under different assumptions, enabling a correct estimation of the train ends when targets get close. Future work would involve focusing on improving the estimation of the length of the train, particularly in scenarios where measurements during track initiation are highly noisy.

References

[1] Y. Bar-Shalom and T. E. Fortmann, *Tracking and Data Association*. Academic Press, 1988.

[2] K. Granström, M. Baum, and S. Reuter, "Extended Object Tracking: Introduction, Overview and Applications," *J. Adv. Inf. Fusion*, vol. 12, no. 2, pp. 139–174, 2017.

[3] T. Broida and R. Chellappa, "Estimating the kinematics and structure of a rigid object from a sequence of monocular images," *IEEE Transactions on Pattern Analysis and Machine Intelligence*, vol. 13, no. 6, pp. 497–513, Jun. 1991.

[4] J. C. Dezert, "Tracking maneuvering and bending extended target in cluttered environment," in *Signal and Data Processing of Small Targets 1998*, vol. 3373. SPIE, Sep. 1998, pp. 283–294.

[5] D. Salmond and N. Gordon, "Group and extended object tracking," in *IEE Colloquium on Trget Tracking: Algorithms and Applications (Ref. No. 1999/090, 1999/215)*, Nov. 1999, pp. 16/1–16/4.

[6] L. Hammarstrand, M. Lundgren, and L. Svensson, "Adaptive Radar Sensor Model for Tracking Structured Extended Objects," *IEEE Transactions on Aerospace and Electronic Systems*, vol. 48, no. 3, pp. 1975–1995, Jul. 2012.

[7] S. Bordonaro, P. Willett, Y. Bar-Shalom, M. Baum, and T. Luginbuhl, "Extracting speed, heading and turn-rate measurements from extended objects using the EM algorithm," in *2015 IEEE Aerospace Conference*, Mar. 2015, pp. 1–12.

[8] R. P. S. Mahler, *Advances in Statistical Multisource-Multitarget Information Fusion*. Artech House, 2014.

[9] J. L. Williams, "Marginal multi-Bernoulli filters: RFS derivation of MHT, JIPDA, and association-based MeMBer," *IEEE Transactions on Aerospace and Electronic Systems*, vol. 51, no. 3, pp. 1664–1687, 2015.

[10] Á. F. García-Fernández, J. L. Williams, K. Granström, and L. Svensson, "Poisson multi-Bernoulli mixture filter: direct derivation and implementation," *IEEE Transactions on Aerospace and Electronic Systems*, vol. 54, no. 4, pp. 1883–1901, 2018.

[11] K. Granström, M. Fatemi, and L. Svensson, "Poisson multi-Bernoulli mixture conjugate prior for multiple extended target filtering," *IEEE Transactions on Aerospace and Electronic Systems*, p. 1, 2019.

[12] Y. Xia, K. Granström, L. Svensson, M. Fatemi, Á. F. García-Fernández, and J. L. Williams, "Poisson Multi-Bernoulli Approximations for Multiple Extended Object Filtering," *IEEE Transactions on Aerospace and Electronic Systems*, vol. 58, no. 2, pp. 890–906, Apr. 2022.

[13] Á. F. García-Fernández, J. L. Williams, L. Svensson, and Y. Xia, "A Poisson Multi-Bernoulli Mixture Filter for Coexisting Point and Extended Targets," *IEEE Transactions on Signal Processing*, vol. 69, pp. 2600–2610, 2021.

[14] M. Fontana, Á. F. García-Fernández, and S. Maskell, "Data-driven clustering and Bernoulli merging for the Poisson multi-Bernoulli mixture filter," *IEEE Transactions on Aerospace and Electronic Systems*, pp. 1–14, 2023.

[15] D. Hill, "Distributed acoustic sensing (DAS): Theory and applications," in *Frontiers in Optics 2015*. Optica Publishing Group, 2015.

[16] M. Briers, S. Maskell, and M. Philpott, "Two-Dimensional Assignment with Merged Measurements using Lagrangian Relaxation," *Proceedings of SPIE - The International Society for Optical Engineering*, vol. 5204, Dec. 2003.

[17] D. Svensson, M. Ulmke, and L. Hammarstrand, "Multitarget Sensor Resolution Model and Joint Probabilistic Data Association," *IEEE Transactions on Aerospace and Electronic Systems*, vol. 48, no. 4, pp. 3418–3434, Oct. 2012.

[18] M. Beard, B.-T. Vo, and B.-N. Vo, "Bayesian Multi-Target Tracking With Merged Measurements Using Labelled Random Finite Sets," *IEEE Transactions on Signal Processing*, vol. 63, no. 6, pp. 1433–1447, Mar. 2015.

[19] Á. F. García-Fernández, L. Svensson, J. L. Williams, Y. Xia, and K. Granström, "Trajectory Poisson multi-Bernoulli filters," *IEEE Transactions on Signal Processing*, vol. 68, pp. 4933–4945, 2020.

[20] A. S. Rahmathullah, Á. F. García-Fernández, and L. Svensson, "Generalized optimal sub-pattern assignment metric," in *Proc. 20th Int. Conf. Information Fusion (Fusion)*, Jul. 2017, pp. 1–8.